SCIENCE CHINA
Physics, Mechanics & Astronomy

• Research Paper •

December 2011 Vol.54 No.12: 2271–2283
doi: 10.1007/s11433-011-4530-7

Establishment of a new tropospheric delay correction model over China area

SONG ShuLi[1*], ZHU WenYao[1], CHEN QinMing[1] & LIOU YueiAn[2]

[1] *Shanghai Astronomical Observatory, Chinese Academy of Sciences, Shanghai 200030, China;*
[2] *Center for Space and Remote Sensing Research, National Central University, Taiwan, China*

Received May 30, 2011; accepted September 5, 2011; published online October 26, 2011

The tropospheric delay is one of the main error sources for radio navigation technologies and other ground- or space-based earth observation systems. In this paper, the spatial and temporal variations of the zenith tropospheric delay (ZTD), especially their dependence on altitude over China region, are analyzed using ECMWF (European Centre for Medium-Range Weather Forecast) pressure-level atmospheric data in 2004 and the ZTD series in 1999–2007 measured at 28 GPS stations from the Crustal Movement Observation Network of China (CMONC). A new tropospheric delay correction model (SHAO) is derived and a regional realization of this model for China region named SHAO-C is established. In SHAO-C model, ZTD is modeled directly by a cosine function together with an initial value and an amplitude at a reference height in each grid, and the variation of ZTD along altitude is fitted with a second-order polynomial. The coefficients of SHAO-C are generated using the meteorology data in China area and given at two degree latitude and longitude interval, featuring regional characteristics in order to facilitate a wide range of navigation and other surveying applications in and around China. Compared with the EGNOS (European Geostationary Navigation Overlay Service) model, which has been used globally and recommended by the European Union Wide Area Augmentation System, the ZTD prediction (in form of spatial and temporal projection) accuracy of the SHAO-C model is significantly improved over China region, especially at stations of higher altitudes. The reasons for the improvement are: (1) the reference altitude of SHAO-C parameters are given at the average height of each grid, and (2) more detailed description of complicated terrain variations in China is incorporated in the model. Therefore, the accumulated error at higher altitude can be reduced considerably. In contrast, the ZTD has to be calculated from the mean sea level with EGNOS and other models. Compared with the direct estimation of ZTD from the 28 GPS stations, the accuracy of the derived ZTD using the SHAO-C model can be improved by 60.5% averagely compared with the EGNOS model. The overall bias and rms are 2.0 and 4.5 cm, respectively, which should be sufficient to satisfy the requirements of most GNSS navigation or positioning applications in terms of the tropospheric delay correction.

EGNOS, GPS, tropospheric delay, SHAO-C model, ECMWF pressure-level data

PACS: 91.10Fc, 91.10Pp, 91.10Xa

1 Introduction

The tropospheric refraction is a well known major error source for earth observation and a variety of radio navigation technologies. The total tropospheric delay consists of hydrostatic (also termed dry) delay and wet delay. They are closely related to the atmospheric pressure and precipitable water vapor respectively [1–4]. Therefore the tropospheric delay can indicate the weather and climate processes and is an important parameter of the atmospheric studies [5–7]. Tropospheric delay is approximately two meters at the zenith direction for the propagating radio signal, and becomes higher as the propagating direction deviates from the zenith towards the horizon direction [8]. The effect of tropospheric

*Corresponding author (email: slsong@shao.ac.cn)

delay may reach 10 m in GNSS positioning if not corrected properly. For GNSS static positioning, in the post-processing mode using sophisticated positioning software (such as GAMIT software), the zenith tropospheric delay is treated as an unknown parameter and estimated through a random process method, resulting in significantly improved positioning precision in the vertical direction to that of the horizontal achieving sub-centimeter level of accuracy [9–12]. However, for the majority of GNSS real-time navigation users, deriving a universal real-time tropospheric delay model (i.e. prediction model) that is easy to use and applicable to different navigation positioning accuracies, has always been actively pursued in order to satisfy the needs for the applications of worldwide GNSS systems, including Compass system [13–15].

The two traditional tropospheric delay models, the Hopfield model and the Saastamoinen model, can be used to calculate the atmospheric delay at an arbitrary station based on the provided surface meteorological parameters and the rate of change with respect to height [16,17]. Nevertheless, as both models require real-time meteorological parameters for their calculations (since using standard parameters results in poor accuracy), it is obvious that they are not perfect for the real-time navigation users. In addition, the temperature lapse rate and water vapor decline rate are regarded as a single global average constant in these two models. This is incompatible with the actual atmosphere situation and could adversely affect the accuracy of the tropospheric delay. Qu et al. [18] also found that the accuracy of the Hopfield model decreased with the increasing altitude of the station.

Collins et al. [13] introduced UNB2(University of New Brunswick) model which is based on the Saastamoinen model, taking into account the major changes in water vapor profiles with latitude. In that model, the pressure, temperature, water vapor pressure, temperature lapse rate, water vapor pressure decline rate, and the average value of these five meteorological parameters are provided on the mean sea level for each latitude band. However, the variation of meteorological parameters over time is not given. With the U.S. standard atmosphere data in 1966, the UNB3 model was established. The average value of the five meteorological parameters and the annual changes amplitude were derived. The global latitude is grouped in 15-degree increments, and users could apply their own latitude and time to calculate the required meteorological parameters with the cosine function and to determine the atmospheric delays.

Similar to the UNB3 model, the European Union recommended the EGNOS (European Geostationary Navigation Overlay Service) model, which is derived from the data of 1°×1° grid of the European Centre for Medium-Range Weather Forecast (ECMWF) [19]. The EGNOS model provided five meteorological parameters for each 15-degree latitude band on the mean sea level, which is the same as UNB3. According to the latitude and the day of year, users can derive their own required meteorological parameters using the cosine function in order to calculate the tropospheric zenith delays. The EGNOS model is recommended by the European Union Wide Area Augmentation System and is now widely used in some practical tropospheric delay models [15,20,21].

Those models are of the type of global average tropospheric delay models, which only reflect the global tropospheric profile of temporal changes while lack of the details of the regional tropospheric features. Therefore it is insufficient to describe the zenith delay variations at regional or local scale. Another issue is that those models do not offer necessary treatment for the elevation and location dependent meteorological conditions and the initial parameter setting at the mean sea level, which could result in poor accuracy of the calculated ZTD in some areas with higher altitude (such as the western region of China). They are not yet perfect for the high accuracy requirements of the real-time positioning users.

In this paper, based on our previous study in Chen et al. [22], using the ZTD sequence measured over several years by the Crustal Movement Observation Network of China (CMONC) and ECMWF pressure-level atmospheric data over China, the spatial and temporal variations of ZTD were analyzed in order to characterize the localized annual cycles on a long-time scale. A new tropospheric delay correction model (SHAO) is constructed referred to as SHAO-C where 'C' stands for China. The SHAO-C model considers the impact of the varying topography in China with a high resolution of regional characteristics. Using direct observations based on GPS ZTD as the ground truth, the ZTD prediction accuracy of SHAO-C model significantly outperforms that of EGNOS over China region. The improvement in accuracy is significantly pronounced in those elevated areas.

2 Characteristics of ZTD in China

2.1 The temporal characteristics of ZTD

In order to establish a tropospheric delay correction model with China regional characteristics, we took the advantage of continuous time series of the measured ZTDs at 28 GPS base stations in CMONC over China areas in years 1999–2007 (Figure 1), and then analyzed the quantitative characteristics of their spatial and temporal variations in different seasons. The GPS data are processed using the GAMIT software [23], and the ZTDs are calculated at a 2 h interval for each station. Figure 2 shows the time series of the ZTDs of four representative stations over a 9-year period. The spectral analysis shows that the time series of ZTDs exhibit the well known annual signal, which can be described by a cosine function as explained in Figure 3, but the other periodic terms such as monthly signal are not so pronounced, as described by [7,24,25].

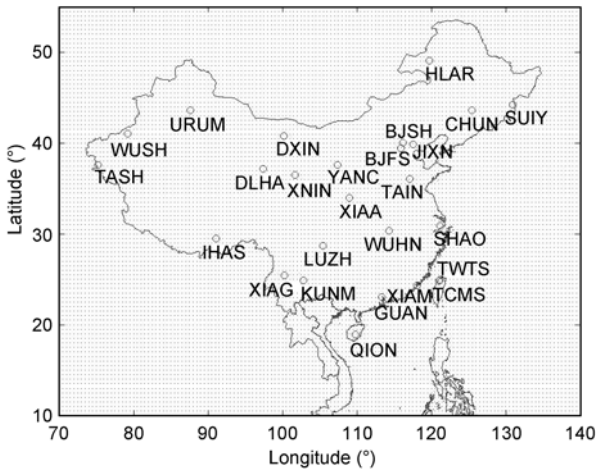

Figure 1 GPS stations and ECMWF grids over China and its surrounding area.

Through an examination of the ZTD variations along longitude and latitude over China regions, it is clearly observed that the spatial variations of the ZTDs primarily depend on the latitude and altitude of the GPS stations, and have much less correlation with longitude. For example, the magnitude of ZTD is greater in the southern and eastern areas generally, which is consistent with the fact that these areas are wetter in the atmosphere and lower in altitude. Furthermore, the regional distribution of the ZTDs shows an increased trend towards the eastern regions associated with a decreasing altitude as showed in Table 1. The four stations have almost the same latitude at different longitudes and altitudes. For SHAO and WUHN almost at the same latitude and altitude with about a 7 degree longitude difference, there're the same mean seasonal value and amplitude of ZTD, and the mean annual ZTD absolutely. For LUZH and LHAS which are also very close to the same latitude, the difference of ZTD is only caused by the altitude.

2.2 Variations of ZTD with altitude

In order to study the dependence of ZTD on altitude, the

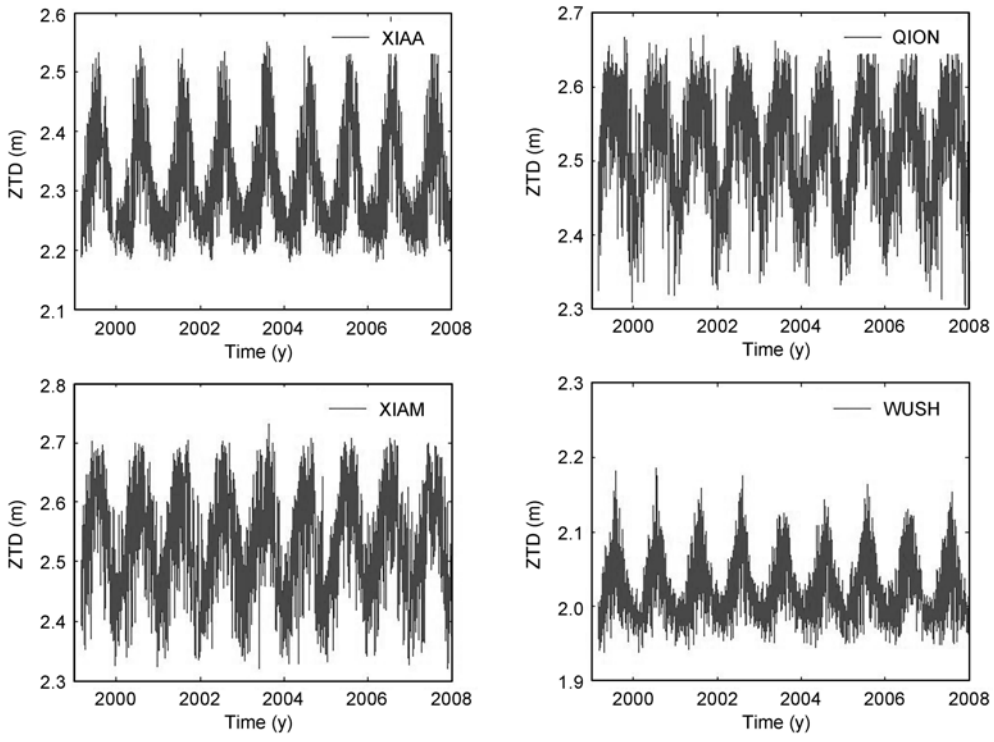

Figure 2 Time series of ZTDs in XIAA (Xi'an), QION (Qiongzhou), XIAM (Xiamen) and WUSH (Wushi) GPS stations.

Table 1 The seasonal mean value and amplitude of ZTD, annual mean ZTD (unit:m) at SHAO,WUHN, LUZH, LHAS stations

Site name	Longitude (deg)	Latitude (deg)	Altitude (meter)	ZTD (Spring)	ZTD (Summer)	ZTD (Autumn)	ZTD (Winter)	Mean amplitude	Mean ZTD
SHAO	121.2	30.9	22.0	2.46	2.59	2.49	2.42	0.09	2.49
WUHN	114.3	30.4	25.8	2.47	2.59	2.49	2.42	0.09	2.49
LUZH	105.6	28.7	298.1	2.41	2.53	2.45	2.36	0.09	2.44
LHAS	91.1	29.5	3622.0	1.53	1.61	1.54	1.50	0.05	1.55

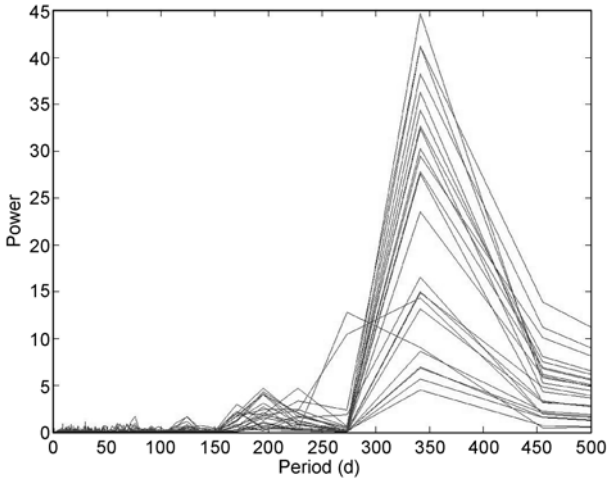

Figure 3 Spectral analysis power of the GPS ZTD series from the GPS stations in CMONC used in this article.

ECMWF pressure-level meteorological data are used for the variation analysis. They are, in particular, the pressure-level ECMWF meteorological data, i.e., 60 pressure levels data of horizontal resolution of 0.5°×0.5° and time resolution of 6 h (http://www. ecmwf.int). Specifically speaking, we use pressure-level atmosphere pressure, temperature, and humidity in the latitude range from 15°N to 54.5°N, and longitude range from 70°E to 139.5°E. The floor grid is shown in Figure 1. The applicability and accuracy of the ECMWF data in China used to be investigated by Chen et al. [22] and Andrei et al. [26]. The assessments show that the bias between GPS ZTD (served as ground truth) and ECMWF ZTD by the integration method ranged from 11.5 mm to −28.6 mm with an average of −10.5 mm, while the largest rms is 35.4 mm with an average of 24.3 mm. These results demonstrate the acceptable accuracy and advantage of establishing the ZTD prediction model over China for navigation and positioning with ECMWF data [22].

With the pressure, temperature, and specific humidity provided by pressure-level ECMWF data at a potential height within each grid, and according to eq. (1) which establishes the relationship between refractive index and meteorological parameters, the refractive index within each cubic box can be calculated as follows:

$$N = k_1(P-e)/T + k_2 \times e/T + k_3 \times e/T^2,$$
$$e = h \times P/0.622, \tag{1}$$

k_1=77.604 K/Pa, k_2=64.79 K/Pa, k_3=377600.0 K^2/Pa, where N is the total refraction, P is the atmospheric pressure, e is the water vapor pressure, and h is the specific humidity. After the total refraction is calculated, the following integral method is used to calculate the ZTD$_i$ in each cubic box:

$$\mathrm{ZTD}_i = 10^{-6}\int_S N\mathrm{d}s = 10^{-6}\sum_i N_i \Delta s_i, \tag{2}$$

where N_i is the atmosphere refractive index in the ith-cubic box, and Δs_i is the height in the ith-cubic box.

With the above ZTD$_i$ in each cubic box, its association with height variation can be characterized over all grid points. Figure 4 shows the variation of the ZTD with increasing height in Kunming, Shanghai, Beijing, and Lhasa as examples.

It can be seen from Figure 4 that the ZTD changes with altitude and shows quadratic characteristics, which can be expressed by the following formula:

$$Z(\varphi, D, h) = Z(\varphi, D, h_0) + a_1(\varphi, D, h_0) \times (h - h_0) + a_2(\varphi, D, h_0) \times (h - h_0)^2, \tag{3}$$

where a_1 and a_2 are the decreasing rate and acceleration of ZTD, respectively; φ, h are the latitude and height of the measured point, respectively, D is the day of year (Doy) at the observing epoch, h_0 is the reference height on which the parameters are given for the $Z(\varphi, D, h_0)$ calculation, and the $Z(\varphi, D, h_0)$ and $Z(\varphi, D, h)$ are the ZTDs calculated at

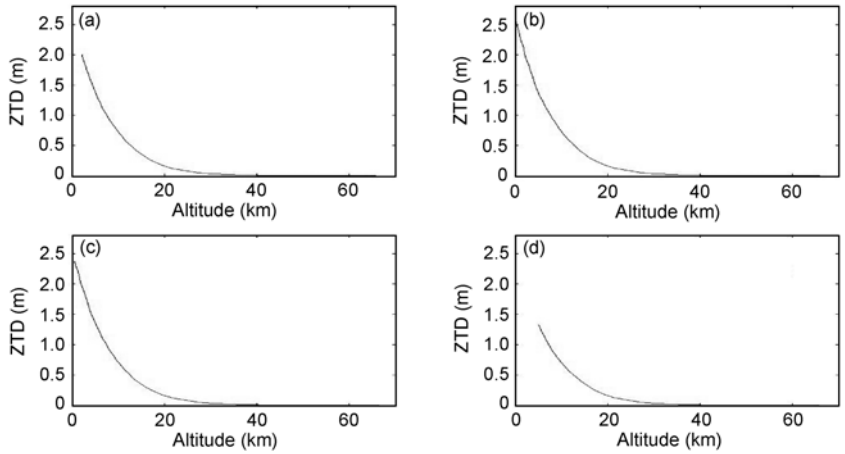

Figure 4 Variations of ZTD with height in KUNM (Kunming, (a)), SHAO (Shanghai, (b)), BJFS (Beijing, (c)), and LHAS (Lhasa, (d)).

the reference height and the user's height, respectively.

In order to study the temporal and spatial variation of a_1, a_2 over China areas, the layered troposphere delays on each grid point of ECMWF in the year 2004 are analyzed. The decreasing rate a_1 and acceleration a_2 are both fitted at a 6-hour interval for each grid point. Figure 5 shows the time series a_1, a_2 for several grid points on the basis of evenly distributed latitude and longitude. It can be seen from Figure 5 that both a_1, a_2 vary slightly during the year, and are basically stable. The temporal correlation coefficients of a_1 and a_2 on each grid point is analyzed as shown in Figure 6. It is found that the correlation coefficient is above 0.95 for a_1 and mostly over 0.9 for a_2, except for some points in summer. Subsequently, the average values of a_1, a_2 are calculated from the 6-hour interval sequence at each grid point. The average values are used as the coefficients of our new tropospheric delay model.

3 Establishment of SHAO-C model

3.1 Determination of model form

Based on the analysis of the temporal and spatial characteristics of ZTD, the initial form of our model is defined as follows:

$$Z(\varphi, D, h_0) = Z_0(\varphi, h_0) - \Delta Z_0(\varphi) \times \cos\left(\frac{2\pi(D - D_{\min})}{365.25}\right), \quad (4)$$

$$Z(\varphi, D, h) = Z(\varphi, D, h_0) + a_1 \times (h - h_0) + a_2 \times (h - h_0)^2, \quad (5)$$

$$a_1 = \mathrm{d}Z(\varphi, D, h)/\mathrm{d}h, \quad a_2 = \mathrm{d}^2 Z(\varphi, D, h)/\mathrm{d}h^2, \quad (6)$$

where h_0 is the average height of each grid in km, $Z_0(\varphi, h_0)$ is the average zenith delay on average height at each grid in m, $\Delta Z_0(\varphi)$is the amplitude of zenith delay on average height at each grid in m, a_1 is the decreasing rate of zenith delay with height at each grid in m/km, a_2 is the decreasing acceleration of zenith delay with height at each grid in $(\mathrm{cm/km})^2$, and D is the day of year (Doy). In the northern hemisphere, $D_{\min}$ = 28 and in the southern hemisphere, $D_{\min}$=211, the coefficients of SHAO-C (h_0, $Z_0(\varphi, h_0)$, $\Delta Z_0(\varphi)$, a_1, a_2) are with the resolutions of 2°×2° in China and its surrounding areas. In general, the model requires the following input parameters: longitude, latitude, height of user, and time (Doy). At first, according to the preliminary coordinate of user, the coefficients of SHAO-C model can be interpolated

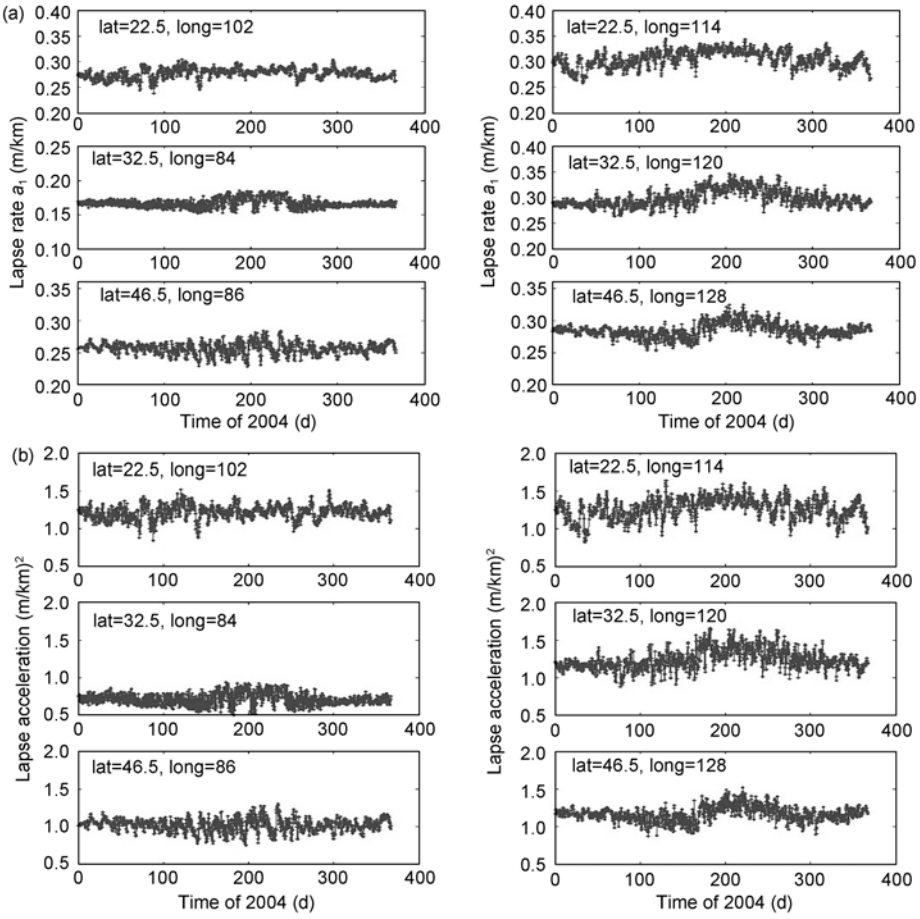

Figure 5 Time series of the decreasing rate (a) and acceleration (b) on several grid points.

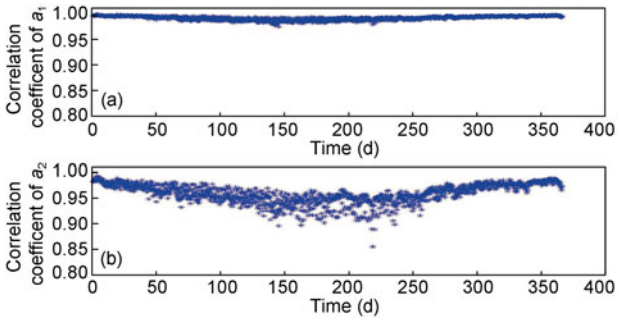

Figure 6 Correlation diagrams of the decreasing rate (a) and acceleration (b) in 2004.

to the user's position, and the initial ZTD correction can be calculated for the user's coordinate improvement. Therefore, with the iterative step, according to the improved coordinate, the updated ZTD correction can be obtained and the new coordinate can be calculated.

3.2 Determination of the SHAO-C model coefficients

Using ECMWF pressure-level data around China region in 2004, the coefficients of SHAO-C model are derived in each grid, including the following five parameters: h_0, $Z_0(\varphi, h_0)$, $\Delta Z_0(\varphi)$, a_1, a_2. The list of coefficients is provided more accurately along the smaller latitude range in China, which is the more accurate reflection of spatial distribution of atmospheric delay.

Figures 7–11 show the five coefficients in China and the surrounding areas. The average height h_0 in each grid is determined according to the bottom level altitude of ECMWF pressure level data. As seen, the variation of the average $Z_0(\varphi, h_0)$ at h_0 height is exactly adverse to the h_0, and the decreasing rates a_1 have the same shape as h_0, which reflects the decreasing variation of atmosphere density with the increasing altitude. The ZTD amplitude $\Delta Z_0(\varphi)$ and decreasing acceleration a_2 also change along with the height of each grid.

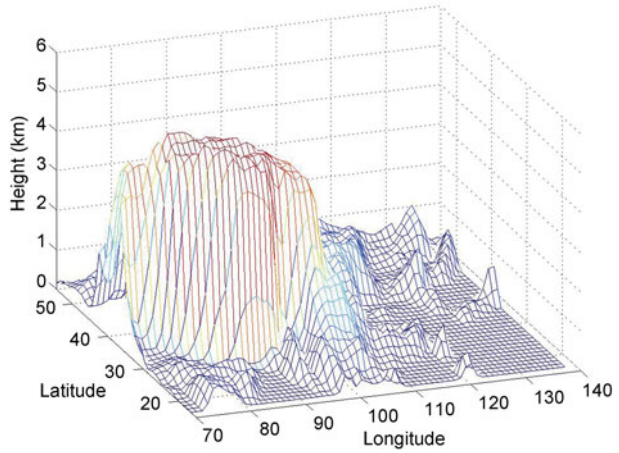

Figure 7 Average height h_0 in each grid of the SHAO-C model in China and the surrounding areas.

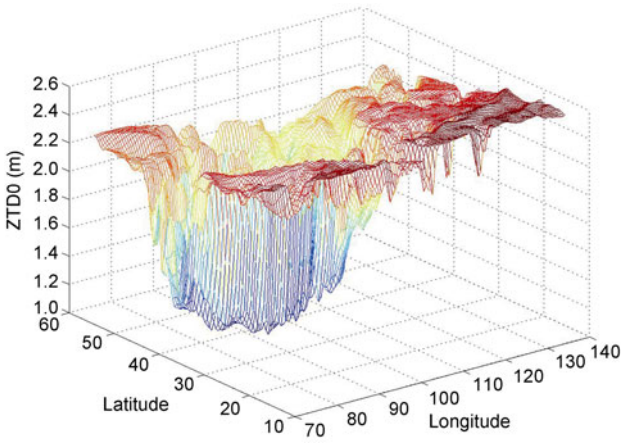

Figure 8 Average $Z_0(\varphi, h_0)$ in each grid of the SHAO-C model in China and the surrounding areas.

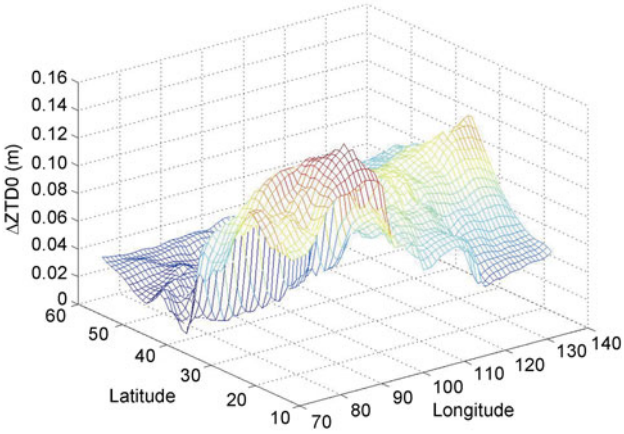

Figure 9 ZTD amplitude $\Delta Z_0(\varphi)$ in each grid of the SHAO-C model in China and the surrounding areas.

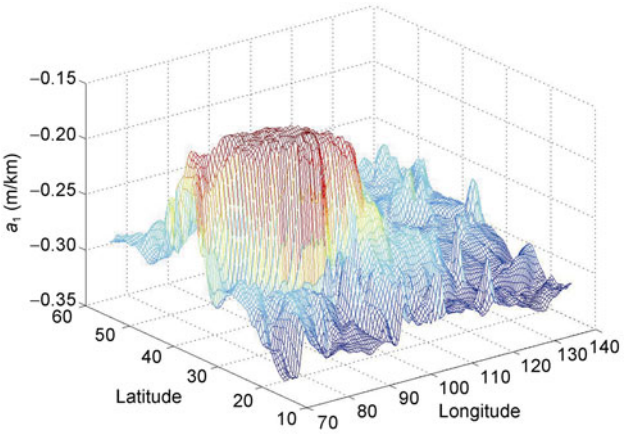

Figure 10 ZTD decreasing rate a_1 in each grid of the SHAO-C model in China and the surrounding areas.

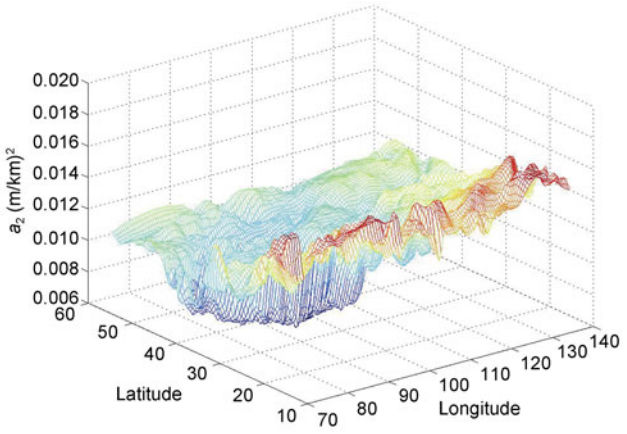

Figure 11 ZTD decreasing acceleration a_2 in each grid of the SHAO-C model in China and the surrounding areas.

4 Assessment of SHAO-C model precision

At present, the accuracy of ZTD measured by GPS base stations is up to 1–2 cm or even better [9,11,27]. GPS ZTD can be regarded as the ground truth to assess the accuracy of other tropospheric delay correction models [22,26]. With the time series of ZTD estimated using CMONC network during the year 2005–2007, the accuracy of SHAO-C model is comprehensively analyzed. The bias and rms are calculated according to the year, month and day respectively, which indicates the reliability of the model.

4.1 Sequence comparison

The comparison of ZTD time series from GPS, SHAO-C and EGNOS model are shown in Figure 12. In Figure 12, the green sequence represents ZTD time series measured by GPS, the blue one from the EGNOS model, and the red one represents the ZTD time series of the SHAO-C model. When the three-year ZTD time series is examined, the resemblance of ZTD between the SHAO-C model and GPS is obviously closer than that between the EGNOS model and GPS. This is because the SHAO-C model provides the

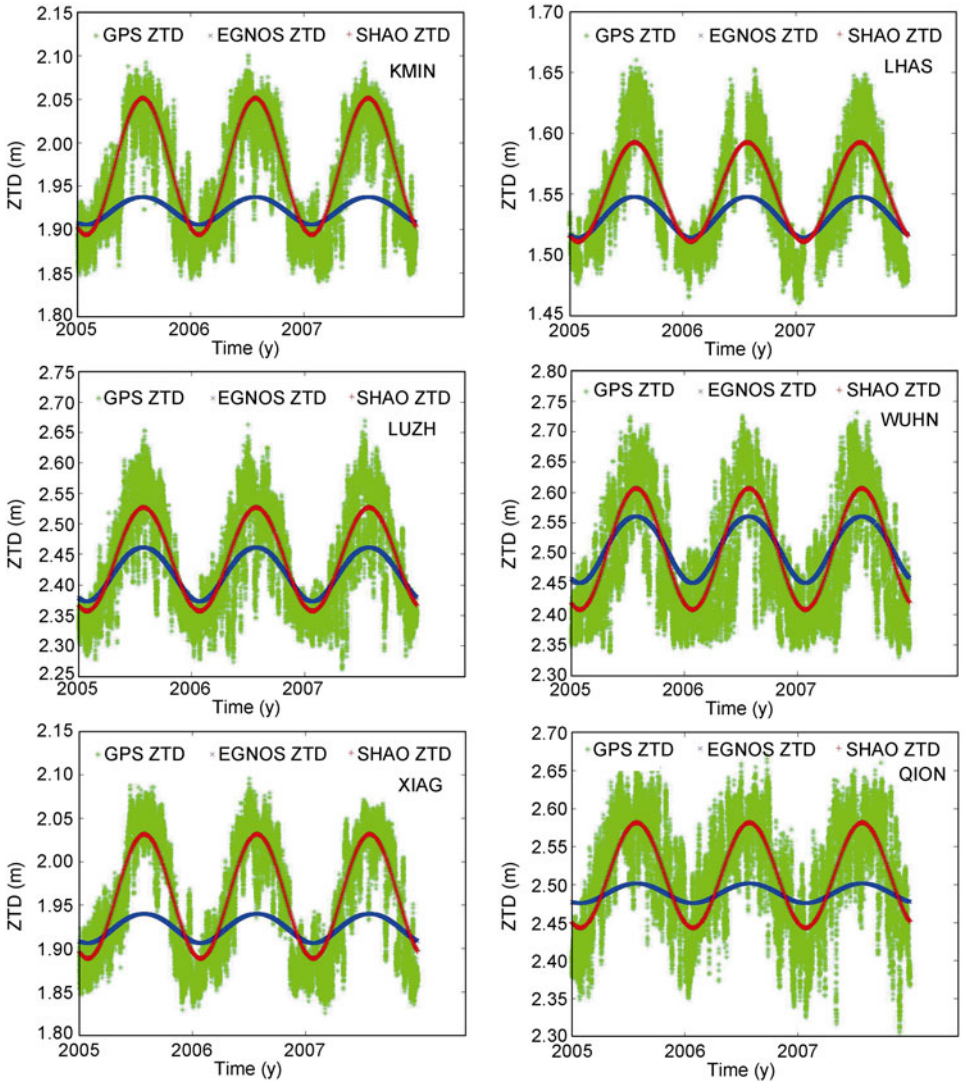

Figure 12 Comparison of the zenith delay among the SHAO-C model, the EGNOS model and GPS measured ZTD.

average height of each grid and the coefficients are given on the average height instead of the mean sea level as in EGNOS and other models. In addition, the model includes the decreasing rates and decreasing acceleration. Therefore, it is no longer necessary to calculate ZTD from the mean sea level by SHAO-C model. This will significantly reduce the accumulated error because of the height difference between the user altitude and the reference height in the model. This is a greater improvement than EGNOS and other models, especially for the areas with relatively high altitude such as Lhasa, Kunming, Xiaguan and so on, as showed in Figure 12. The difference between ZTD prediction values of the SHAO-C model and the GPS measurements do not exceed 10 cm for the three-year period.

Besides the direct ZTD time series comparison of SHAO-C and EGNOS models, the residuals and monthly and daily precision with respect to GPS ZTD are also compared as shown in Figure 13 using KMIN station as an example. With respect to GPS ZTD, the residuals of SHAO-C model are mostly less than 5 cm, even in summer. There's no obvious difference over different seasons. However, the residuals of EGNOS model in summer are particularly large, up to 15 cm. The same is true in monthly and daily statistics. The monthly biases and rms of EGNOS model are in the range from −3 to −10 cm and 2 to 11 cm, while only about 0–3 cm and 2–5 cm in the SHAO-C case with significantly reduced variation over different seasons. Similar cases can also be found at many other stations such as XIAG, LHAS, QION, and WUHN, as listed in Tables 2 and 3 where the average monthly biases and rms at individual stations over the 2005–2007 period are shown.

4.2 Monthly statistics

Here we examine some details of the average monthly bias/rms of EGNOS and SHAO-C models over the 2005–2007 period at each station as showed in Tables 2 and 3. In each column, the left row is for EGNOS and the right row for SHAO-C. From Tables 2 and 3, we can see that:

(1) With all the 28 stations included, the biases of EGNOS model are in the range of 0.1–11.5 cm, with the mean value of 3.7 cm. The maximum bias is at GUAN station in June. The rms range from 1.1 to 12.1 cm and the maximum rms of 5.4 cm is again at GUAN station in June. For the SHAO-C model, the biases are in the range of 0.1–6.9 cm and rms of 1.2–9.3 cm with the mean bias of 2.0 cm and mean rms of 4.2 cm respectively. The maximum bias and rms are both at BJFS station in July.

(2) 70% station-month bias is improved for the SHAO-C model at 28 stations in 12 months, and the improvements are from 0 to 99.7%, and the mean is 60.5%.

(3) In July, August and September, the bias is reduced

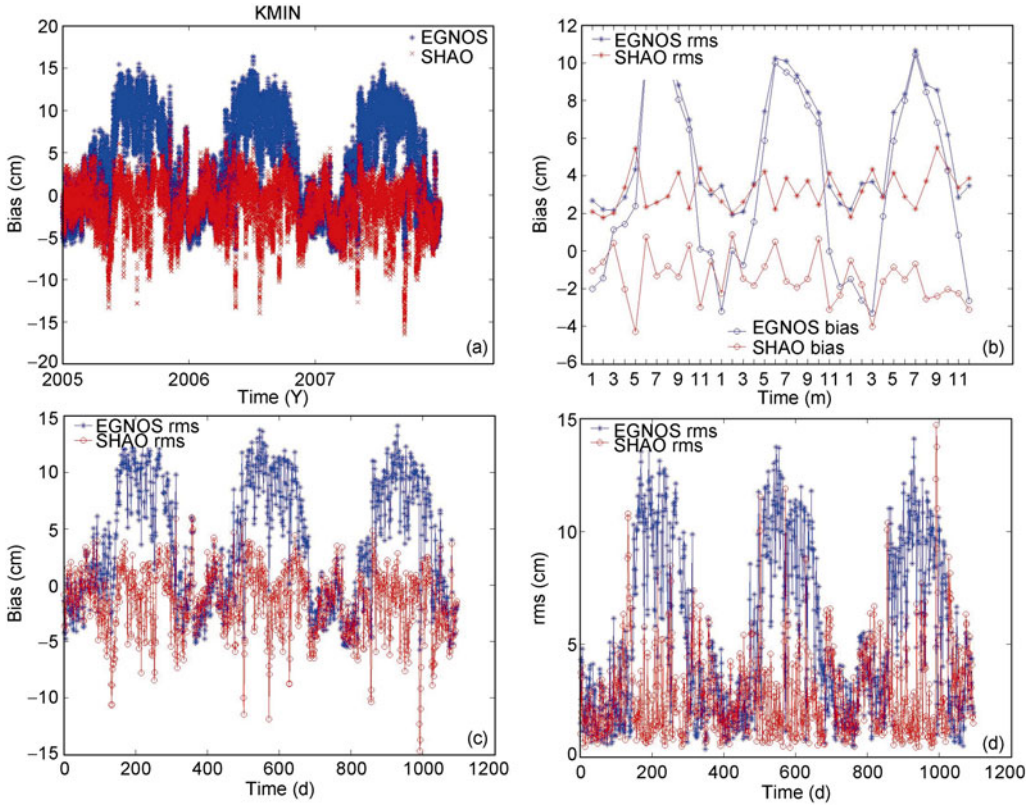

Figure 13 The ZTD comparison of SHAO-C and EGNOS models with respect to GPS between 2005–2007 at KMIN station: (a) difference of ZTD, (b) bias and rms statistics in one month, (c) bias in everyday and (d) rms in everyday.

Table 2 Average monthly bias between 2005–2007 at each station, with the unit of cm (In each column, the left row is for EGNOS and the right row for SHAO-C)

Site	1		2		3		4		5		6		7		8		9		10		11		12	
BJFS	–4.4	1.8	–4.7	1.6	–7.2	–0.9	–9.1	–3.0	–7.3	–1.9	–3.0	1.4	3.1	6.9	2.8	6.6	–4.3	0.3	–6.4	–0.9	–8.3	–2.2	–6.3	0.0
BJSH	–3.7	1.9	–3.8	1.8	–6.2	–0.5	–8.2	–2.7	–6.7	–2.0	–2.1	1.5	3.5	6.4	3.1	6.1	–3.7	0.0	–5.9	–1.2	–7.4	–1.9	–5.3	0.4
CHUN	–1.7	2.3	–2.3	1.8	–4.6	–0.6	–6.2	–2.6	–5.1	–2.5	–0.3	1.0	3.5	4.0	3.8	4.3	–2.7	–1.3	–5.2	–2.6	–5.6	–2.0	–3.4	0.6
DLHA	–0.7	–1.1	–0.8	–1.2	–1.0	–1.5	–1.2	–2.0	–1.1	–2.5	1.6	–0.5	4.1	1.7	3.9	1.5	1.2	–0.7	–0.5	–1.8	–1.5	–2.3	–1.1	–1.6
DXIN	–1.9	–0.5	–2.5	–1.0	–3.5	–1.6	–5.3	–2.8	–6.0	–3.4	–5.5	–3.0	–1.1	1.2	–1.9	0.5	–3.6	–1.1	–4.7	–2.0	–4.6	–2.2	–3.1	–1.3
GUAN	–4.2	–0.9	–0.4	2.7	1.6	3.5	5.0	4.7	7.3	4.4	11.5	6.3	6.7	0.1	6.7	0.1	5.2	0.4	1.5	–1.1	–3.0	–3.0	–5.3	–3.2
HLAR	–0.4	1.8	–1.4	0.9	–3.5	–0.8	–5.6	–2.9	–5.9	–3.6	–2.0	–0.7	1.7	2.4	–0.5	0.3	–3.5	–2.1	–5.4	–3.1	–5.1	–2.4	–2.5	0.1
HRBN	–1.4	2.3	–2.1	1.5	–4.8	–0.9	–6.4	–2.7	–5.8	–2.8	–1.2	0.8	2.9	4.1	1.8	3.2	–3.2	–1.1	–6.2	–3.1	–6.0	–2.3	–3.4	0.4
JIXN	–4.0	2.0	–4.1	1.9	–6.6	–0.6	–8.4	–2.8	–6.9	–2.3	–2.5	1.0	3.1	5.8	2.8	5.6	–4.1	–0.5	–6.3	–1.5	–7.7	–2.1	–5.7	0.3
KMIN	–2.2	–1.3	–1.4	–0.5	–1.0	–1.7	1.6	–1.8	4.7	–2.0	9.4	–0.1	9.9	–1.2	9.2	–1.8	7.5	–1.8	5.9	–0.4	0.3	–2.8	–1.6	–2.0
LHAS	–1.9	–1.7	–1.2	–1.1	–0.8	–1.1	–0.2	–1.5	1.8	–0.7	3.4	–0.2	5.8	1.4	6.8	2.5	4.7	1.1	0.8	–1.6	–1.5	–2.8	–2.0	–2.1
LUZH	–3.4	–1.9	–1.9	–0.4	–1.6	–1.0	–0.5	–1.5	1.7	–1.4	5.9	0.8	8.8	2.4	6.8	0.5	4.6	–0.3	3.6	0.7	–1.5	–2.2	–3.1	–2.4
QION	–5.6	–2.5	–3.1	–0.2	0.2	1.7	3.1	2.1	5.6	1.7	7.5	1.1	6.3	–1.5	7.9	0.3	6.7	0.6	2.8	–0.7	–0.3	–1.0	–1.9	–0.2
SHAO	–4.4	0.1	–3.0	1.6	–5.1	–1.0	–6.4	–3.5	–2.0	–0.5	1.5	1.0	7.4	6.0	4.6	3.1	2.8	2.4	–3.3	–1.6	–4.8	–1.7	–5.8	–1.7
SUIY	–1.9	2.2	–2.3	1.7	–4.8	–0.9	–5.4	–2.1	–4.1	–2.1	–0.1	0.5	3.7	3.3	4.7	4.4	–1.7	–1.0	–5.4	–3.2	–5.7	–2.3	–3.7	0.2
TAIN	–4.4	1.7	–3.8	2.2	–5.8	–0.5	–6.6	–2.8	–5.8	–4.1	–2.6	–3.0	4.9	3.3	4.9	3.3	–1.3	–1.5	–4.3	–2.4	–6.7	–2.8	–5.5	–0.2
TASH	0.6	–1.5	0.8	–1.3	0.6	–1.6	0.5	–2.1	1.1	–2.3	1.2	–3.0	2.3	–2.4	2.9	–1.8	1.0	–3.1	0.2	–3.1	–0.4	–3.0	0.1	–2.1
URUM	–1.2	–3.2	–1.4	–3.4	–2.3	–3.3	–2.4	–2.9	–3.3	–3.2	–2.4	–2.4	–0.5	–0.5	–2.9	–2.9	–4.1	–4.0	–3.6	–3.6	–3.2	–3.7	–2.3	–3.5
WUHN	–4.7	–0.5	–2.9	1.3	–4.6	–1.2	–4.9	–3.3	–3.1	–3.9	0.7	–2.4	7.3	2.9	5.0	0.7	0.6	–2.2	–3.2	–3.7	–6.2	–4.3	–6.4	–2.9
WHJF	–4.5	–0.4	–2.7	1.4	–4.3	–1.2	–4.7	–3.4	–3.7	–4.8	0.9	–2.5	7.5	2.7	5.5	0.8	1.0	–2.2	–2.9	–3.7	–6.0	–4.4	–6.3	–3.1
WUSH	–0.8	–2.7	–0.6	–2.4	–0.8	–2.3	–2.6	–3.8	–2.3	–3.6	–1.6	–3.2	0.5	–1.4	0.1	–1.8	–0.7	–2.3	–1.7	–3.0	–2.2	–3.5	–1.6	–3.2
XIAA	–3.8	0.1	–3.4	0.5	–4.4	–1.1	–5.6	–3.6	–3.7	–3.5	–1.7	–3.4	6.6	3.8	6.0	3.3	1.6	0.1	–1.4	–1.0	–5.2	–3.1	–4.9	–1.5
XIAG	–3.3	–1.8	–1.9	–0.4	–1.8	–1.7	0.3	–1.9	3.7	–1.4	7.9	0.4	9.8	0.9	9.1	0.3	7.9	0.6	4.9	0.2	–1.3	–3.2	–3.2	–2.8
XIAM	–3.2	–0.1	0.1	3.0	0.7	2.5	3.5	3.1	6.3	3.3	10.2	4.8	5.3	–1.4	8.4	1.8	5.5	0.4	1.8	–0.9	–1.1	–1.2	–3.6	–1.6
XNIN	–1.3	–0.4	–1.3	–0.4	–1.2	–0.7	–1.0	–1.4	0.2	–1.6	2.3	–0.7	5.7	1.9	6.2	2.4	3.4	0.5	0.9	–0.6	–1.9	–2.2	–1.9	–1.3
YANC	–2.7	0.1	–2.9	–0.2	–3.7	–1.1	–5.3	–3.5	–4.2	–3.5	–2.5	–2.9	2.9	1.7	2.8	1.6	–0.3	–0.6	–2.6	–1.7	–4.7	–2.7	–3.9	–1.3
YONG	–4.7	0.2	–3.6	1.0	–1.5	1.6	0.8	1.2	4.9	2.5	7.5	2.2	6.9	0.2	8.5	1.6	7.1	2.1	1.7	–0.5	–3.4	–2.1	–0.6	2.5
ZHNZ	–4.9	–0.1	–4.1	0.7	–5.8	–2.1	–6.8	–5.2	–5.2	–6.3	–2.7	–6.4	6.3	1.0	4.8	–0.5	0.2	–3.2	–3.9	–4.7	–6.9	–5.0	–6.0	–2.1
Mean	2.9	1.3	2.3	1.4	3.2	1.4	4.2	2.7	4.3	2.8	3.6	2	4.9	2.6	4.8	2.3	3.4	1.3	3.5	2	4	2.7	3.6	1.6
rms	3.3	1.6	2.6	1.6	3.8	1.6	5	2.9	4.7	3	4.8	2.6	5.6	3.2	5.4	2.9	4	1.7	4	2.3	4.7	2.8	4	1.9

more obviously, with the mean reductions of 2.3, 2.5 and 2.1 cm, respectively. The maximum improvements of biases are 8.9, 8.8 and 7.3 cm in those three months. Among all the statistics, the maximum improvement of bias is 9.3 cm in June at KMIN station.

(4) The rms are also improved much more in July, August and September, with the mean reductions of rms being 1.3, 1.6 and 1.7 cm, respectively. The maximum reduction values of rms are 7.2, 7.5 and 6.9 cm in the three months. The maximum reduction of rms is 7.5 cm at XIAG in July out of all the rms statistics.

Based on the study of the monthly average statistics at 28 stations in 12 months, the accuracy of SHAO-C model is improved at most stations and in most months. Especially in summer, the superiority of SHAO-C model is more distinct.

4.3 Annual statistics

The accuracy of SHAO-C model with respect to the GPS measured ZTD at 28 GPS stations in China is analyzed annually. From the statistics in Figure 14, the annual biases of SHAO-C model in 2005–2007 three years are mostly less than 2 cm at most stations. However, the annual bias of EGNOS model at most stations is greater than 2 cm. It should be noted that there is no obvious correlation between the bias and the station elevation. On the other hand, the rms' is negatively correlated with the station elevation as shown in Figure 15. That can be explained by the fact that the atmosphere is thinner at higher altitude stations. Table 4 shows the specific annual rms and bias of ZTD forecast by the SHAO-C model and the EGNOS model from 2005 to 2007 compared with the GPS measured ZTD, and the mean value of bias and rms from all stations are given in the last line of Table 4.

Table 4 and Figures 14 and 15 show the following three points. (1) Based on the annual rms and bias statistics, the accuracy as well as the precision of the SHAO-C model are superior to EGNOS. This is because the SHAO-C model

Table 3 Average monthly rms between 2005–2007 at each station, with the unit of cm (In each column, the left row is for EGNOS and the right row for SHAO-C)

Site	1		2		3		4		5		6		7		8		9		10		11		12	
BJFS	4.7	2.2	5.1	2.6	7.7	2.8	9.5	4.2	9.2	6.1	6.2	5.5	7.0	9.3	6.9	9.0	6.6	5.1	7.6	4.1	8.7	3.3	6.6	1.8
BJSH	3.9	2.3	4.2	2.6	6.7	2.6	8.6	3.9	8.5	5.8	5.7	5.4	7.0	8.8	7.2	8.8	6.1	4.8	6.9	3.9	7.7	2.9	5.5	1.7
CHUN	2.1	2.6	2.7	2.2	5.0	2.1	6.5	3.5	6.4	4.5	4.5	4.5	6.1	6.3	8.3	8.4	4.8	4.2	6.0	3.8	5.9	2.8	3.8	1.7
DLHA	1.2	1.5	1.3	1.6	1.4	1.8	1.8	2.4	2.2	3.1	3.0	2.6	5.3	3.9	4.9	3.4	3.1	2.9	1.8	2.5	1.8	2.4	1.4	1.8
DXIN	2.3	1.4	2.9	1.8	4.0	2.4	5.7	3.4	6.6	4.3	6.3	4.3	5.4	5.3	4.9	4.5	4.9	3.6	5.0	2.8	4.8	2.6	3.3	1.7
GUAN	5.4	3.7	3.7	4.7	4.8	5.5	6.9	6.6	9.8	7.7	12.1	7.5	8.1	4.9	8.0	4.8	8.0	6.0	5.2	4.7	7.4	7.3	7.5	6.2
HLAR	1.5	2.3	2.1	1.8	3.9	1.8	5.9	3.4	6.3	4.3	4.3	3.8	4.7	5.0	3.8	3.7	4.3	3.2	5.7	3.6	5.4	3.0	2.8	1.4
HRBN	1.8	2.6	2.5	2.1	5.2	2.2	6.8	3.4	6.7	4.3	4.4	4.3	5.8	6.5	6.4	6.8	5.0	4.0	6.7	4.0	6.3	2.9	3.7	1.6
JIXN	4.2	2.3	4.5	2.7	7.1	2.7	8.9	4.1	8.7	5.8	5.8	5.2	6.7	8.3	7.1	8.5	6.2	4.7	7.4	4.2	8.1	3.3	5.9	1.9
KMIN	2.8	2.2	2.6	2.3	2.7	3.0	3.1	3.2	6.4	4.6	9.7	2.5	10.3	2.9	9.6	3.2	8.6	4.5	6.8	3.0	3.3	4.0	3.0	3.4
LHAS	2.3	2.1	1.5	1.5	1.5	1.8	1.9	2.4	2.8	2.3	4.3	2.6	6.1	2.4	7.0	3.1	5.2	2.4	2.3	2.5	2.2	3.2	2.2	2.4
LUZH	3.8	2.5	3.0	2.4	3.3	3.1	4.2	4.4	6.6	6.3	8.0	5.4	10.3	6.0	8.1	4.7	8.0	6.5	5.2	3.5	3.4	3.7	3.6	3.0
QION	6.6	4.4	5.1	4.0	3.8	4.1	5.1	4.5	7.6	5.3	8.2	3.6	7.4	4.3	8.5	3.0	8.2	4.8	6.0	5.2	5.6	5.6	5.1	4.7
SHAO	6.2	4.2	4.8	4.1	8.0	6.2	8.9	7.2	8.7	8.5	7.0	6.6	9.5	8.4	7.2	6.5	4.7	3.6	7.8	7.1	7.9	6.4	7.2	4.6
SUIY	2.3	2.6	2.8	2.3	5.3	2.4	5.8	3.0	5.2	3.8	3.5	3.5	6.1	5.9	8.4	8.1	4.3	4.1	6.0	4.1	6.0	3.0	4.1	1.9
TAIN	4.7	2.3	4.4	3.1	6.5	3.2	7.4	4.4	8.0	6.9	7.1	7.0	8.1	7.2	8.3	7.5	7.3	7.5	6.6	5.4	7.3	4.1	6.0	2.4
TASH	1.2	1.8	1.5	1.8	1.4	2.0	1.3	2.4	2.3	3.0	2.3	3.6	3.2	3.2	3.8	3.0	2.3	3.6	1.2	3.3	1.1	3.1	1.2	2.3
URUM	2.0	3.6	1.8	3.6	3.2	4.0	3.6	3.9	4.4	4.4	4.1	4.1	4.0	4.0	4.7	4.7	5.0	5.0	4.1	4.1	3.8	4.2	2.6	3.7
WUHN	5.9	3.5	5.0	4.4	6.4	4.6	7.6	6.6	8.4	8.7	7.4	7.6	8.5	5.3	7.7	5.9	7.6	7.9	6.9	7.1	8.5	7.3	7.3	4.7
WHJF	5.7	3.5	5.0	4.4	6.2	4.6	7.4	6.6	8.4	9.0	7.5	7.6	8.7	5.2	7.8	5.6	7.7	8.0	6.8	7.1	8.4	7.4	7.3	4.8
WUSH	1.4	2.9	1.8	2.9	2.0	2.9	3.2	4.3	3.6	4.5	3.3	4.3	2.8	3.1	3.2	3.7	2.6	3.4	2.7	3.6	2.8	3.9	2.0	3.4
XIAA	4.3	2.0	4.2	2.6	5.1	3.0	6.7	5.2	6.9	6.9	6.8	7.3	9.1	7.4	8.2	6.5	7.1	7.0	5.3	5.0	6.0	4.2	5.3	2.6
XIAG	3.8	2.6	3.0	2.3	3.1	3.1	2.3	2.9	5.2	3.9	8.3	2.8	10.1	2.6	9.4	2.5	8.6	3.5	6.3	3.4	3.7	4.4	3.9	3.8
XIAM	5.3	4.2	4.0	5.1	5.0	5.5	6.3	6.0	9.3	7.4	11.3	6.9	7.3	5.3	9.3	4.5	8.3	5.9	5.0	4.5	6.0	5.9	6.3	5.5
XNIN	1.8	1.2	2.0	1.6	1.9	1.7	2.0	2.3	2.5	2.9	3.6	2.8	6.7	4.3	7.1	4.3	4.7	3.3	2.6	2.4	2.3	2.5	2.1	1.6
YANC	3.0	1.4	3.4	1.8	4.1	2.2	5.6	4.0	5.6	5.1	5.2	5.3	5.8	5.4	6.0	5.6	4.5	4.6	4.4	3.8	4.9	3.2	4.0	1.8
YONG	7.4	5.7	5.0	4.0	5.3	5.3	4.8	4.9	7.2	5.6	8.1	3.9	7.7	3.7	9.0	3.6	8.6	5.7	4.3	3.8	7.0	6.3	5.4	5.6
ZHNZ	5.4	2.2	4.8	2.6	6.5	3.9	7.7	6.4	8.0	8.8	7.4	9.2	8.8	6.3	7.4	5.8	7.5	8.3	6.7	7.0	7.7	6.1	6.4	3.3
Mean	3.7	2.7	3.4	2.8	4.5	3.2	5.6	4.3	6.5	5.5	6.3	5.0	7.0	5.4	7.1	5.3	6.1	4.9	5.3	4.3	5.5	4.2	4.5	3.0
rms	4.1	2.9	3.6	3	4.9	3.5	6	4.5	6.8	5.8	6.7	5.3	7.3	5.7	7.3	5.7	6.4	5.2	5.6	4.5	5.9	4.5	4.9	3.3

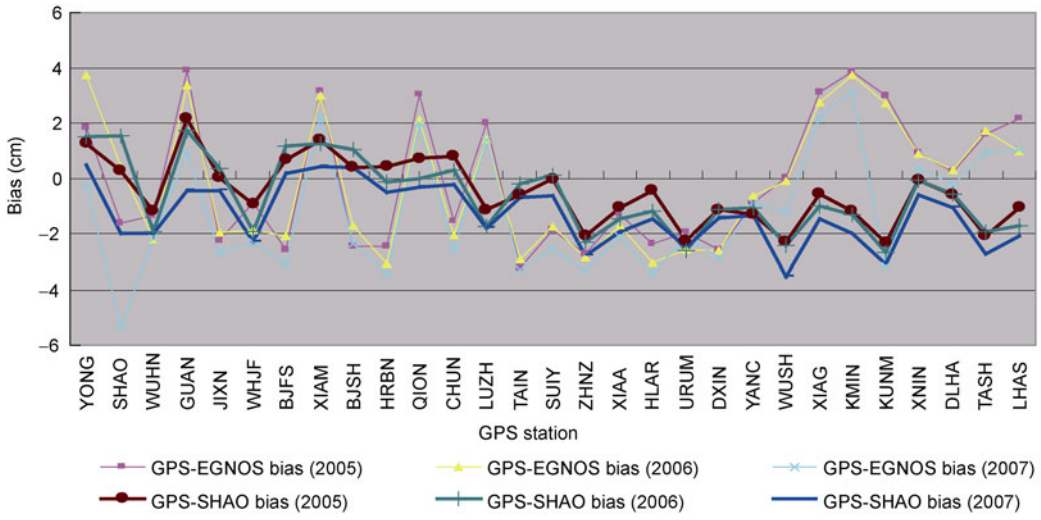

Figure 14 Annual statistics of bias (GPS ZTD-SHAO/EGNOS ZTD) (stations sorted by height).

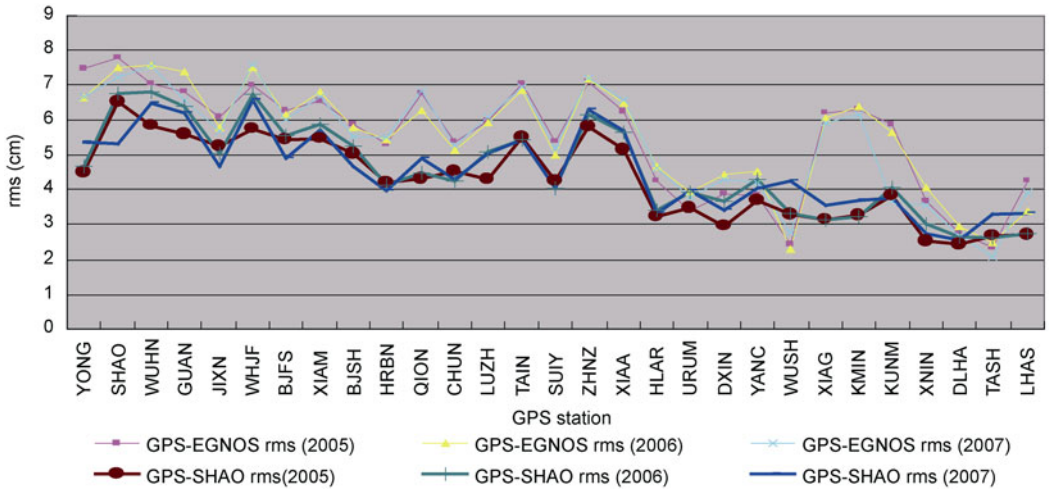

Figure 15 Annual statistics of rms (GPS ZTD-SHAO/EGNOS ZTD) (stations sorted by height).

Table 4 Bias and rms (GPS ZTD-EGNOS/SHAO ZTD) in the year 2005–2007 (unit: cm)

GPS site name	Altitude (m)	GPS ZTD - EGNOS ZTD						GPS ZTD - SHAO ZTD					
		2005		2006		2007		2005		2006		2007	
		bias	rms	bias	rms	bias	rms	bias	rms	bias	rms	bias	rms
YONG	10	1.8	7.5	3.7	6.7	–0.3	6.7	1.2	4.5	1.5	4.7	0.5	5.4
SHAO	22	–1.6	7.8	0.4	7.5	–5.3	7.2	0.3	6.5	1.6	6.8	–1.9	5.3
WUHN	26	–1.3	7	–2.2	7.6	–2.2	7.5	–1.1	5.8	–1.9	6.8	–1.9	6.5
GUAN	31	4.1	7.7	3.4	8.3	0.7	7.3	2.2	5.6	1.8	6.4	–0.4	6.2
JIXN	39	–4.1	7.1	–3.8	6.8	–4.6	6.9	0.6	5.3	0.9	5.1	0.2	4.6
WHJF	72	–0.9	7	–1.9	7.5	–2.3	7.6	–1	5.8	–1.9	6.7	–2.3	6.6
BJFS	87	–4.6	7.4	–4.1	7.2	–5.1	7.4	0.8	5.5	1.3	5.6	0.3	4.9
XIAM	106	3.2	7.2	3	7.4	2.3	7.4	1.5	5.5	1.3	5.9	0.5	5.7
BJSH	155	–4.2	6.9	–3.4	6.6	–4.1	6.6	0.5	5	1.2	5.3	0.6	4.7
HRBN	198	–2.5	5.3	–3.1	5.4	–3.4	5.5	0.5	4.2	–0.1	4.1	–0.5	4
QION	208	3	6.8	2.1	6.3	2	6.9	0.7	4.3	–0.1	4.5	–0.3	4.9
CHAN	268	–2	5.6	–2.5	5.3	–3	5.5	0.7	4.5	0.2	4.3	–0.4	4.3
LUZH	298	2	6.1	1.5	6.1	1.4	6.2	–0.2	4.1	–0.8	4.8	–0.8	4.8
TAIN	339	–3.2	7.1	–2.9	6.9	–3.3	6.9	–0.7	5.5	–0.3	5.4	–0.8	5.4
SUIY	369	–2	5.5	–1.9	5.1	–2.7	5.3	0.2	4.3	0.3	4.1	–0.4	4
ZHNZ	444	–2.7	7.1	–2.8	7.2	–3.3	7.2	–2.5	6	–2.8	6.3	–3.2	6.5
XIAA	509	–1.3	6.3	–1.7	6.5	–2.1	6.6	–0.4	5.1	–0.8	5.5	–1.2	5.5
HLAR	629	–2.3	4.2	–3	4.6	–3.4	4.6	–0.3	3.2	–1	3.4	–1.3	3.2
URUM	859	–2.3	3.5	–2.8	4.1	–2.4	3.9	–2.8	3.8	–3.1	4.3	–3	4.3
DXIN	1018	–3.6	4.6	–3.6	5.1	–3.8	5	–1.3	3	–1.4	3.7	–1.6	3.5
YANC	1304	–2.3	4.5	–2.1	5.1	–2.4	4.9	–1.3	3.7	–1	4.3	–1.3	4
WUSH	1395	–0.7	2.6	–0.9	2.5	–2	3.2	–2.3	3.3	–2.5	3.3	–3.5	4.3
XIAG	1974	3.1	6.4	2.7	6.3	2.2	6.2	–0.5	3.1	–0.9	3.1	–1.4	3.5
KMIN	1986	3.8	6.5	3.7	6.6	3.1	6.4	–1.1	3.2	–1.3	3.2	–2	3.7
KUNM	1986	3	6.1	2.7	5.9	–3.8	4.2	–2.3	3.8	–2.6	4	–3.1	3.7
XNIN	2364	1.1	3.7	1	4.1	0.5	3.6	–0.2	2.5	–0.2	3	–0.7	2.8
DLHA	2956	0.4	2.8	0.4	3	–0.1	2.7	–0.9	2.5	–0.8	2.7	–1.3	2.7
TASH	3049	1.1	2.1	1.2	2.2	0.4	2	–2.1	2.7	–1.9	2.6	–2.7	3.3
LHAS	3622	2.3	4.3	1.1	3.4	1.2	4	0	2.5	–0.6	2.2	–1	2.8
mean	908	–0.4	5.7	–0.5	5.8	–1.6	5.7	–0.4	4.3	–0.5	4.5	–1.2	4.5

directly uses the starting height of the grid nearest to user's position. (2) The accuracy and precision of SHAO-C model are relatively uniform over time and location. (3) The rms of SHAO-C model reduces along with the increased station elevation. This is because the moisture in the atmosphere becomes less at higher altitude locations. Thus less modeling errors will be introduced. (4) For 28 GPS Stations, the overall average rms of ZTD predicted by the SHAO-C model over three years is around 4.5 cm, with a maximum at SHAO (Shanghai) less than 7 cm. This should be adequate for satisfying the demands of most of the navigation or surveying applications.

5 Disscussion

In the above sequence, and daily, monthly and annual comparisons with commonly used models, such as EGNOS, the SHAO-C model exhibits much better performance, because it takes the localized characteristics of the tropospheric zenith delays into consideration over China region with the following features.

(1) Model parameters given on the average height of each grid. The reference height of model parameters is given at the average height of each grid, which avoids calculating from the mean sea level as required by the EGNOS model and other models. This greatly eliminates the accumulative error during the integration process when the target position is at a higher altitude. The model takes the characteristics of terrain variations into consideration in China region. In the western area of China, the accuracy of the model is significantly better than EGNOS. Therefore, the model will positively impact the navigation and positioning applications in China.

(2) Higher spatial resolution. The resolution of the parameters of SHAO-C model is 2°×2°, which is much finer than the 15° grid interval of EGNOS model. This higher spatial resolution can better represent the regional characteristics of tropospheric conditions, especially for western China with complicated terrains.

(3) Direct modelling of the zenith tropospheric delay. In the SHAO-C model, the atmosphere zenith delay is directly modeled, which simplifies the algorithm and the setup of model parameters. Thus it is more convenient to correct tropospheric delay for general navigation and positioning users. It also sets the basis to refine and further optimize the model parameters through densification, namely by introducing more GPS zenith delay time series from global and Chinese stations.

There is still work to do to further improve the model, such as to extend the coefficients to global area, to inspect its accuracy with different grid resolutions of model coefficients. We will present our future research findings in the mentioned area.

6 Conclusions

For navigation and general surveying applications, there are a few available tropospheric correction models, such as UNB3, EGNOS, of which the model parameters are given on the mean sea level resulting in increased biases at locations of higher altitudes. For better serving the navigation and surveying needs in a general way, the SHAO-C model for China area has been established in this work and the coefficients of SHAO-C model in China area are derived with the meteorology data over the corresponding region. In the SHAO-C model, the reference altitude of SHAO-C parameters is given at the average height of each grid, and a more detailed description of complicated terrain variations in China is incorporated in the model. In comparison with the EGNOS model, the ZTD prediction accuracy of the SHAO-C model is significantly improved over China region, especially at stations of higher altitudes. Compared with the direct estimation of ZTD from the 28 GPS stations of CMONC, the accuracy of the derived ZTD using the SHAO-C model can be improved by 60.5% averagely than the EGNOS model. The overall bias and rms are 2.0 and 4.5 cm respectively, and the maximum error is less than 10 cm, which should be sufficient to satisfy the requirements of most GNSS navigation or positioning applications in terms of the tropospheric delay correction.

The authors thank ECMWF and CMONC for providing the data. This work was supported by the National Natural Science Foundation of China (Grant No. 10603011 and 41174023), the National High Technology Research and Development Program of China (Grant No. 2009AA12Z307), Science and Technology Commission of Shanghai Municipality (Grant Nos. 05QMX1462 and 08ZR1422400), and the Youth Foundation of Knowledge Innovation Project of the Chinese Academy of Sciences, Shanghai Astronomical Observatory (Grant No. 5120090304).

1 Tregoning P, Boers R, O'Brien D. Accuracy of absolute precipitable water vapor estimates from GPS observations. J Geophys Res, 1998, 103: 701–710
2 Liou Y A, Huang C Y. GPS observation of PW during the passage of a typhoon. Earth Planets Space, 2000, 52: 709–712
3 Manuel H P, Juan J M, Sanz J. A new strategy for real-time integrated water vapor determination in WADGOPS networks. Geophy Res Lett, 2001, 28: 3267–3270
4 Song S L, Zhu W Y, Ding J C, et al. 3D water-vapor tomography with Shanghai GPS network to improve forecasted moisture field. Chin Sci Bull, 2006, 51: 607–614
5 Trenberth K E. Seasonal variations in global sea level pressure and the total mass of the atmosphere. J Geophys Res, 1981, 86: 5238–5246
6 Liou Y A, Teng Y T, Hove T V, et al. Comparison of precipitable water observations in the near tropics by GPS, microwave radiometer, and radiosondes. J Appl Meteor, 2001, 40: 5–15
7 Jin S G, Park J, Cho J, et al. Seasonal variability of GPS-derived zenith tropospheric delay (1994–2006) and climate implications. J Geophys Res, 2007, 112: D09110
8 Zhang J, Lachapelle G. Precise estimation of residual tropospheric delays using a regional GPS network for RTK applications. J Geod,

2001, 75: 255–266
9 Fang P, Bevis M, Bock Y, et al. GPS meteorology: Reducing systematic errors in geodetic estimates for zenith delay. Geophys Res Lett, 1998, 25: 3583–3586
10 Ge M, Calais E, Haase J. Reducing satellite orbit error effects in near real-time GPS zenith tropospheric delay estimation for meteorology. Geophys Res Lett, 2000, 27: 1915–1919
11 Snajdrova K, Boehm J, Willis P, et al. Multi-technique comparison of tropospheric zenith delays derived during the CONT02 campaign. J Geod, 2005, 79: 613–623
12 Tregoning P, Herring T A. Impact of a priori zenith hydrostatic delay errors on GPS estimates of station heights and zenith total delays. Geophys Res Lett, 2006, 33: L23303
13 Collins J P, Langley R B. Limiting factors in tropospheric propagation delay error modeling for GPS airborne navigation. In: The Institute of Navigation 52nd Annual Meeting, Cambridge, Massachusetts, USA, 1996
14 Farah A, Terry M, Chris J H. High Spatial variation tropospheric model for GPS-Data simulation. J Navig, 2005, 58: 459–470
15 Tomislav K, Maja B, Markezic I. Evaluation of EGNOS tropospheric delay model in south-eastern Europe. J Navig, 2009, 62: 341–349
16 Hopfield H S. Tropospheric effect of electromagnetically measured range: Prediction from surface weather data. J Radio Sci, 1971, 6: 357–367
17 Saastamoinen J. Contributions to the theory atmospheric refraction, Part II Refraction corrections in satellite Geodesy. Bull Geod, 1972, 105: 279–298
18 Qu W J, Zhu W Y, Song S L. The evaluation of the precision about Hopfield, Saastamoinen, and EGNOS tropospheric delay correction model. Acta Astron Sin, 2008, 49: 113–122
19 Penna N, Dodson A, Chen W. Assessment of EGNOS tropospheric correction model. J Navig, 2001, 54: 37–55
20 Dodson A H. Assessment of EGNOS troposphere correction model. In: Proceeding of IONGPS-99, the 12th International Meeting of the Satellite Division of The Institute of Navigation, Nashville, Tenn., 1999. 1401–1407
21 Andrea P. Tropospheric zenith wet and hydrostatic delay models for the ESA Galileo testbed: Models based on meteorological measurements and a blind model. In: ION GPS/GNSS, Portland, 2003
22 Chen Q M, Song S L, Stefan H, et al. Assessment of ZTD derived from ECMWF/NCEP data in China. GPS Solut, 2011, doi: 10.1007/s10291-010-0200-x
23 Herring T A, King R W, McClusky S C. Document for the GAMIT GPS analysis software, release 10.3. 2006
24 Humphreys T E, Kelley M C, Huber N, et al. The semidiurnal variation in GPS-derived zenith neutral delay. Geophys Res Lett, 2005, 32: L24801
25 Wang J H, Zhang L Y. Climate application of a global, 2-hourly atmospheric precipitable water dataset derived from IGS tropospheric products. J Geod, 2009, 83: 209–217
26 Andrei C, Chen R. Assessment of time-series of troposphere zenith delays derived from the global data assimilation system numerical weather model. GPS Solut, 2008, 13: 109–117
27 Song S L, Zhu W Y, Ding J C, et al. Near real-time sensing of PWV from SGCAN and the application test in numerical weather forecast. Chin J Geophys, 2004, 40: 719–727